

# Depleted pyrochlore antiferromagnets

Christopher L. Henley

Dept. of Physics, Cornell Univ., Ithaca NY 14853-2501 USA

E-mail: [c1h@ccmr.cornell.edu](mailto:c1h@ccmr.cornell.edu)

**Abstract.** I consider the class of “depleted pyrochlore” lattices of corner-sharing triangles, made by removing spins from a pyrochlore lattice such that every tetrahedron loses exactly one. Previously known examples are the “hyperkagome” and “kagome staircase”. I give criteria in terms of loops for whether a given depleted lattice can order analogous to the kagome “ $\sqrt{3} \times \sqrt{3}$ ” state, and also show how the pseudo-dipolar correlations (due to local constraints) generalize to even the random depleted case.

Consider “bisimplex” antiferromagnets [1], meaning that *every* spin is shared between exactly two triangles or tetrahedra. Let there be only the nearest-neighbour coupling, so the system is highly frustrated. After the kagomé [2], pyrochlore [3, 4], and garnet [5] lattices, further such systems were discovered such as the “kagomé staircase” (realised in e.g.  $\text{Ni}_3\text{V}_2\text{O}_8$  [6]) and the “hyperkagomé” lattice [8, 7] (realised in  $\text{Na}_4\text{Ir}_3\text{O}_8$  [9]). Both magnetic lattices are obtained from the pyrochlore lattice by removing 1/4 of the sites so as to leave a network of corner-sharing triangles. This paper considers the entire family of such “depleted” structures, and the equilibrium states of classical or semiclassical spins on them.<sup>1</sup>

The pyrochlore lattice is most simply visualised as the “medial graph” (bond midpoints) of a diamond lattice. A depleted lattice is made by placing a dimer covering on the diamond lattice bonds, then removing spins from the covered sites. This constraint is plausible: in real spinels with magnetic B sites (= a “pyrochlore” magnetic lattice), dilution is achieved by substituting a nonmagnetic species X on B sites. Due to size (or maybe charge) imbalance, X ions repel; hence the lattice gas of X ions maps to an Ising antiferromagnet [3] in a field. That is itself a highly frustrated problem, with a degenerate ground state (all those dimer coverings) – provided the lattice gas has only nearest neighbour interactions. Further neighbour ion terms presumably select a specific depletion pattern.

After some examples of depleted lattices, I address two questions (for the periodic *and* random cases): (i) What is the pattern of magnetic order (if any); (iii) How do we generalize the disordered classical liquid with pseudo-dipolar correlations due to the constraints?

## 1. Regularly depleted pyrochlore lattices

In this section, I catalog some highly symmetrical dimer coverings of the diamond lattice, each of which specifies a different depleted pyrochlore lattice.

<sup>1</sup> I will not consider other depleted lattices, except to observe the hidden symmetry (considering nearest-neighbour bonds) whereby the hyperkagomé lattice [9] is equivalent to a garnet lattice [5], is reminiscent of the hidden equivalence of the 1/5-depleted square lattice of  $\text{CaV}_4\text{O}_9$  [10] to the 4-8 lattice [11].

These can be conveniently be visualized in two possible ways: (i) projecting the conventional cubic cell (containing four diamond sites, i.e. four pyrochlore tetrahedra) in the (100) direction; or, (ii) expressing the diamond lattice as a stacking of puckered honeycomb layers, in which the (odd) sites have an additional bond extending upwards (downwards) to the next layer.

### 1.1. Cubic conventional cell

Consider the family of patterns preserving the periodicity of the conventional cubic cell, with four dimers per cell. There are only three symmetry-inequivalent ways to place them. Pattern 1 has all dimers oriented the same; the diamond lattice separates into disconnected (puckered) honeycomb layers, and the spins form stacks of uncoupled kagomé lattices, as induced by a field in “kagomé ice” [12].

Pattern 2 has two dimers in one orientation and two in another orientation. This again separates the lattice into disjoint slabs, now transverse to a (110) axis. The depleted lattice is a “kagomé staircase”, which has the topology of a kagomé lattice, but folded so the hexagons alternate between two (111) type orientations. Imagine a canonical spinel  $\text{AB}_2\text{O}_4$  with cubic lattice constant  $a_c \approx 8.2 \text{ \AA}$ ; depletion by B-site vacancies gives the formula  $\text{A}_1\text{B}_{1.5}\text{O}_4$  with  $x = 1/4$ . Pattern 2 makes the structure orthorhombic, with  $a \approx a_c/\sqrt{2}$ ,  $b \approx \sqrt{2}a_c$ , and  $c \approx a_c$ . This nearly describes the “kagomé staircase” compounds e.g.  $\text{VCo}_{1.5}\text{O}_4$ , except each successive slab is slid a half cell relative to the one before.

Pattern 3 uses each of the four possible orientations once, yielding the “hyperkagomé” arrangement with cubic symmetry. as realized [9] in the spinel  $\text{Na}_4\text{Ir}_3\text{O}_8$ , i.e.  $(\text{Na}_{1.5})_1(\text{Ir}_{3/4}\text{Na}_{1/4})_2\text{O}_4$  in our framework,

### 1.2. Kagomé layer stacking approach

I will focus on the layered patterns made by viewing the diamond lattice as a stack of puckered honeycomb layers (a kagomé layer of spin sites) connected by vertical linking bonds (forming a triangular lattice). Say a fraction  $x_{\text{link}}$  of linking bonds is depleted; then the honeycomb layer has depletion  $x_{\text{kag}} \equiv (1 - x_{\text{link}})/3$ ; its depletion pattern is a dimer covering having monomers at the endpoints of the depleted linking bonds. If either kind of layer lacks threefold point symmetry, we restore it by stacking the layers with a rotation (producing a screw axis).

**Table 1.** Some depleted lattices, with properties of the shortest loops (Loop density is per site; in the tags, interlayer bonds are underlined for comparison to Fig. 1.)

Fig. 1 part	$x_{\text{link}}$	$x_{\text{kag}}$	$L_{\text{loop}}$	loop density	Colouring tags	Loop is colourable?
a)	1/3	2/9	8	1/2	<i>bbbs<u>bbb</u>b</i>	no
b)	1/4	1/4	10	3/4	<i>(bb<u>sb</u>s)<sup>2</sup></i>	yes
c)	1/4	1/4	8	1/16	<i>bbbb<u>ssb</u></i>	no
d)	1/7	2/7	6	1/14	<i>bb<u>bbb</u>b</i>	yes

Fig. 1 shows some examples; there are many more, e.g. in Fig. 1(c) a different honeycomb dimer pattern could be used. Fig. 1(b) is just the cubic “hyperkagomé” structure. With  $x_{\text{link}} = 0$  and  $x_{\text{kag}} = 1/3$  we get a dimer covering of the honeycomb lattice.

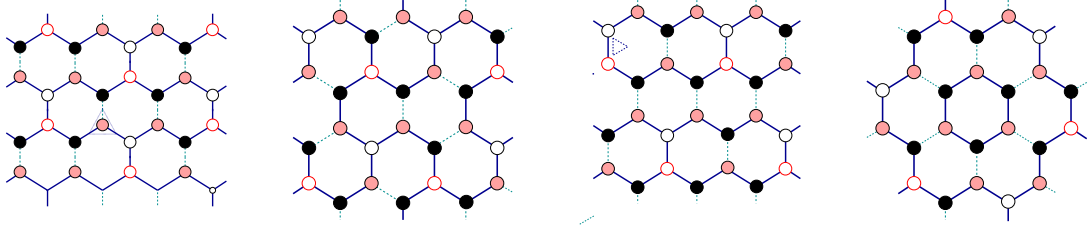


**Figure 1.** Depleted lattices built by stacking puckered layers along a 3-fold axis. Diamond lattice are shown bonds as lines (in the layer) or as circles (for linking bonds: up=shaded, down=black). Removed bonds are indicated by dashed lines or empty circles. In (a) and (c), successive layers are stacked with a  $2\pi/3$  rotation around the dotted triangle. (a). a  $\sqrt{3} \times \sqrt{3}$  pattern; (b). hyperkagomé lattice; (c). another  $2 \times 2$  pattern; (d). a  $\sqrt{7} \times \sqrt{7}$  pattern.

## 2. Magnetic ground state

The magnetic Hamiltonian is assumed to be  $\mathcal{H} = J \sum_{\langle ij \rangle} \mathbf{s}_i \cdot \mathbf{s}_j$  where only nearest-neighbour isotropic interactions are included, and  $\{\mathbf{s}_i\}$  are either classical unit vectors or quantum spins with  $S \gg 1$ . Let us review the known story for the kagomé or garnet/hyperkagomé antiferromagnets. The classical ground states are the (many) configurations in which the spins differ by angles  $2\pi/3$  on every triangle. It then transpires that (i) a (still highly degenerate) subset of “coplanar” states gets selected at harmonic order, which amounts to a 3-colouring; (ii) a specific coplanar ordered state is selected by anharmonic fluctuations, which was the “ $\sqrt{3} \times \sqrt{3}$ ” state in the kagomé case [14, 13, 15] and Lawler’s state in the hyperkagomé/garnet case [7]. Do these results generalise?

### 2.1. Coplanar states

At harmonic order, thermal fluctuations (in the classical case [2, 4]) or quantum fluctuations [13, 16] select “coplanar” ground states, such that spins in different triangles lie in the same plane of spin space.<sup>2</sup> This selection should carry over to arbitrary corner-sharing triangle networks.

A coplanar ground state has every spin in one of three directions so it is effectively a 3-colouring of the sites (equivalently, diamond-lattice bonds) by colours  $A, B, C$ , such that every triangle (i.e. bonds meeting at one diamond vertex) has one of each colour. By König’s theorem [17] of graph theory, a 3-colouring exists on any bipartite graph with coordination  $z = 3$ , and hence on *any* depleted lattice.

Any 3-colouring of a depleted lattice can usefully be reimagined as a 4-colouring of the original pyrochlore lattice, with the fourth color corresponding to the depleted sites. Thus, any 3-colouring in fact generates *four* different ways to build a depleted lattice (along with a sample 3-colouring of each), depending on which color we select for removal. (In Lawler’s state [7], all four colours are equivalent; each colour forms a “trillium” lattice [18].)

### 2.2. Ising mapping and effective Hamiltonian

As is well known, at harmonic order all the coplanar states have equivalent Hamiltonians [2, 13]. Hence, fluctuations distinguish among them only at *anharmonic* order. Observe too that coplanar configurations cannot distinguished on the loop-free “cactus lattice” – the medial graph of a  $z = 3$  Bethe lattice – since they are all symmetry-equivalent by permutations of the sites. *Loops* are essential to state selection [19, 20].

On the kagomé lattice, coplanar states are more transparently represented by “chiralities”  $\eta_\alpha = \pm 1$ , Ising variables defined on triangle centers  $\alpha$ , and equal to  $+1$  ( $-1$ ); if the colours

<sup>2</sup> The constraint counting argument of [4] carries over independent of how the triangles are arranged.

$ABC$  run counterclockwise (clockwise) around the triangle. The colouring can be uniquely reconstructed (modulo trivial symmetries) from  $\{\eta_\alpha\}$ , but not every configuration of  $\{\eta_\alpha\}$  corresponds to a colouring. With approximations, one can obtain an effective Hamiltonian of form  $\mathcal{H}_{\text{eff}} = -\sum_{\alpha\beta} \mathcal{J}_{\alpha\beta} \eta_\alpha \eta_\beta$  in the quantum case [15], and also in the classical case [21] at small  $T$ , based on [22]. The nearest neighbor Ising coupling  $\mathcal{J}_1 < 0$ , so the optimum state is an antiferromagnetic pattern of  $\eta_\alpha$  on the honeycomb vertices.

What about  $d = 3$ ? Let the index  $\alpha$  label triangles, or equivalently diamond-lattice vertices. A gauge choice is necessary on every triangle to define which sense of its normal vector is “up”, before the spin chirality can be defined. I conjecture that, in general, the sign of  $\mathcal{J}_1$  is the opposite of the projection of the normal vectors of the respective triangles.

Then the ground state has an alternating chirality pattern (which is always possible, since the diamond vertices are bipartite). For the hyperkagomé lattice – the most regular depleted example – this gives the correct answer: Lawler’s state, favored in a large- $n$  calculation [7] and found in simulations [8].) Whereas the “ $\sqrt{3} \times \sqrt{3}$ ” state of the kagomé had alternating colours (e.g.  $ABABAB$ ) around loops and triple colors ( $ABCABC\dots$ ) along lines, and has a nonzero ordering vector, Lawler’s state has alternating colours along lines and ordering vector  $Q = 0$ .<sup>3</sup>

The basis for believing  $\mathcal{J}_1 < 0$  is general is that in the kagomé case, it was expressed [15, 21] in terms of expectations of spin-wave fluctuations of “soft” modes, which have only anharmonic-order restoring forces. Such soft modes are generic to the coplanar state on any of our lattices. They sum to zero on every triangle, a “zero-divergence” constraint that implies generic power-law correlations of the fluctuations, whether classical [23, 24, 25] or quantum [15, 26]. We obtain  $\mathcal{J}_1 < 0$  if the sign depends on orientation the same way it does asymptotically. A caveat is that at root, the crucial spin-wave correlations must depend on the loops (as noted above, only loops distinguish among coplanar states); the pseudo-dipolar correlations are just a coarse-grained way to incorporate the net effects of many long loops. An alternate local derivation of  $\mathcal{H}_{\text{eff}}$ , based on a loop expansion [19, 20, 28] might better capture the differences among depleted lattices.

### 2.3. Colourability

Let’s call the lattice “colourable” if there is a 3-colouring satisfying the above rule. That is true if and only if every fundamental loop of diamond-lattice bonds is colourable. Tag the each bond of the loop as “ $s$ ” or “ $b$ ” depending whether the corresponding site is analogous to a “straight” or “bent” point in a path on the kagomé lattice.<sup>4</sup> Surrounding a  $b$  step the colouring alternates (e.g.  $ABA$ ), as in a kagomé hexagon, whereas surrounding an  $s$  step it cycles (e.g.  $ABC$ ), as on a straight line of kagomé. Let  $\{j_1, j_2, \dots\}$  be the steps in the loop tagged  $s$ ; it can be shown the colours are consistent around the loop if and only if  $\sum_m (-1)^{m+j_m} \equiv 0 \pmod{6}$ .<sup>5</sup>

Colourability does not depend on just the loop shape, but also on the orientations of the depleted dimers touching each site of the loop. Consider 6-loops (the shortest that we may have) in one layer (like those shown in Fig. 1): each vertex of the hexagon can be tagged by 0 (if the depleted dimer runs vertical from it) or 1 (if the depleted dimer sticks outwards from the hexagon center). Of the  $2^6$  possible 6-loops,  $45/64$  are not colourable: the seven classes (111000), (111010), (110110), (111110), (110000), (110100), and (111100). The six colourable classes account for  $19/64$  of the 6-loops.

<sup>3</sup> Lawler’s state lacks “weathervane” modes which were sometimes considered as the key feature on the kagomé.

<sup>4</sup> Note that given step  $i$  there is always (at least) one non-depleted direction available at both steps  $i+1$  and  $i-1$ ; if the path enters on one of these but does not leave on the other, it is “bent”, otherwise it is “straight”.

<sup>5</sup> Or you may just start colouring (e.g.  $ABAC\dots$ ) in accordance with the rules mentioned, and see whether the loop ends on the same colour it started with.

### 3. Classical cooperative paramagnet

I first review known properties of random ensembles with divergence-like constraints. Say some bonds of a bipartite  $z$ -coordinated lattice are coloured (with the same colour) such that  $z'$  bonds are coloured at every vertex. Construct a divergence-free vector field by letting every bond have unit flux from the even to the odd endpoint if coloured, or flux  $-z'/(z - z')$  if uncoloured; the local volume average defines a coarse-grained “polarization”  $\mathbf{P}(\mathbf{r})$  with  $\nabla \cdot \mathbf{P} = 0$  [23, 24, 25]. In a random ensemble of such colourings, the entropy density behaves as

$$\sigma(\mathbf{P}) = \sigma_0 - \frac{1}{2}\alpha|\mathbf{P}|^2 + \text{higher order} \quad (1)$$

Combined with the divergence constraint, (1) implies long-range, pseudo-dipolar correlations:

$$\langle P_a(0)P_b(\mathbf{r}) \rangle \propto \frac{d(r_a r_b / |\mathbf{r}|^2) - \delta_{ab}}{\alpha|\mathbf{r}|^d} \quad (2)$$

in  $d$  dimensions. Correlations of the physical degrees of freedom are generally proportional to (2). Dimer models [23] are the case  $z' = 1$ ; ice models are the case  $z = 4$ ,  $z' = 2$ . A  $z$ -colouring produces  $z - 1$  flavours of  $\mathbf{P}(r)$  (one for each colour, minus one linear dependency) hence  $\mathbf{P}(\mathbf{r})$  in that case is a  $d \times (z - 1)$  tensor. The ground states of classical spins on a bisimplex lattice – our original problem – satisfy the constraint  $\sum_{i \in \alpha} \mathbf{s}_i = 0$  [1]; the polarization in that case is a  $d \times m$  tensor where  $m$  is the number of spin components, and here too we expect (2) describes the correlations [8, 24, 25].

The problem at hand is a depleted pyrochlore lattice ( $z = 3$ ) – periodic or random – either with classical  $m = 3$  component spins, or else a 3-colouring: thus,  $\mathbf{P}(\mathbf{r})$  has spin or flavour indices.<sup>6</sup> But I’ll work out, instead, the simpler case of a dimer covering on the depleted lattice; similar results are expected for the real problems.

Let the dimer pattern’s polarization field be  $\mathbf{P}(\mathbf{r})$  on the depleted lattice ( $z = 3$ ), or  $\mathbf{E}(\mathbf{r})$  as a covering of the original ( $z = 4$ ) lattice; and let  $\mathbf{D}(\mathbf{r})$  be the polarization field of the ( $z = 4$ ) dimers defining the depletion pattern. It is trivial to check that

$$\mathbf{P} = \frac{9}{8}(\mathbf{E} + \frac{1}{3}\mathbf{D}). \quad (3)$$

Now, the random depleted lattice is a “quenched” model in which first  $\mathbf{D}$  is fixed according to a single-component ensemble, i.e. Eq. (1) with  $\alpha|\mathbf{P}|^2 \rightarrow \alpha^D|\mathbf{D}|^2$ . But consider, just for now, a random ensemble with two (equivalent) colours of non-overlapping dimers described by  $\mathbf{D}$  and  $\mathbf{E}$ . By cubic lattice symmetry as well as  $\mathbf{D} \leftrightarrow \mathbf{E}$  symmetry, the joint entropy density must be isotropic to quadratic order:

$$\sigma^{DE} = \sigma_0^{DE} - \frac{1}{2}\alpha^{DE}(|\mathbf{D}|^2 + |\mathbf{E}|^2 + 2\lambda\mathbf{D} \cdot \mathbf{E}). \quad (4)$$

where  $0 < \lambda < 1$  is expected. This also must be the entropy density for  $\mathbf{E}$  conditioned on a *frozen* (not untypical)  $\mathbf{D}(\mathbf{r})$ . Using the change of variables (3), the entropy density is (1) with  $\mathbf{P} \rightarrow \tilde{\mathbf{P}} \equiv \mathbf{P} + \tilde{\lambda}\mathbf{D}$   $\alpha \equiv \frac{8}{9}\alpha^{DE}$  and  $\tilde{\lambda} \equiv \frac{9}{8}(\lambda - \frac{1}{3})$ . Thus,  $\mathbf{P}$  is a linear combination of two independent fields  $\tilde{\mathbf{P}}(\mathbf{r})$  and  $\mathbf{D}(\mathbf{r})$ , each having correlations like (2), with respective prefactors  $1/\alpha$  and  $1/\alpha^D$ . On the other hand, a *periodic* depleted lattice has a uniform  $\mathbf{D}(\mathbf{r})$ , offsetting  $\mathbf{P}(\mathbf{r})$  by a constant. Note that, unless a depleted lattice has cubic symmetry or small  $\mathbf{D}$ , the coefficients of  $P_a P_b$  terms become anisotropic, (deriving from  $O(DDEE)$  cross terms in (4)).

<sup>6</sup> The flavour case is the large- $S$  quantum model at temperatures low enough for coplanarity, but high enough to ignore the small energies selecting specific spin patterns [24] as in Sec. 2.2.

#### 4. Conclusion

I have shown there exist many depleted lattices (Sec. 1) and given a picture both of the ordered ground state (in Sec. 2) and the cooperative paramagnet state (Sec. 3). In the latter state, the disconnected correlation function of  $\mathbf{P}(\mathbf{r})$  has the pseudodipolar form (2). Most of the results apply both to regular and random depleted lattices. Random depletion is an inviting way to include just enough constraints to maintain many features of uniform lattices, e.g. satisfying *every* triangle and allowing coplanar ground states, which are violated in rare places in the case of unconstrained site dilution [1].

#### Acknowledgments

I thank M. Lawler and C. Broholm for discussions. This work was supported by NSF Grant No. DMR-0552461.

#### References

- [1] C. L. Henley, Can. J. Phys. 79, 1307 (2001).
- [2] J. T. Chalker, P. C. W. Holdsworth, and E. F. Shender, *Phys. Rev. Lett.*, **68**, 855 (1992).
- [3] P. W. Anderson, Phys. Rev. 102, 1008 (1956).
- [4] R. Moessner and J. T. Chalker, Phys. Rev. B 58, 12049 (1998).
- [5] O. A. Petrenko and D. McK. Paul, Phys. Rev. B 63, 024409 (2000).
- [6] N. Rogado et al., Solid State Commun. 124, 229 (2002);
- [7] M. J. Lawler, H.-Y. Kee, Y. B. Kim, and A. Vishwanath, Phys. Rev. Lett 100, 227201 (2008)
- [8] J. M. Hopkinson, S. V. Isakov, H.-Y. Kee, and Y. B. Kim, Phys. Rev. Lett. 99, 037201 (2007)
- [9] Y. Okamoto et al, Phys Rev Lett 99, 137207 (2007)
- [10] S. Taniguchi *et al*, J. Phys. Soc. Jpn. 64, 2758 (1995).
- [11] K. Sano and K. Takano, J. Phys. Soc. Jpn. 65, 46 (1996).
- [12] K. Matsuhira *et al*, J. Phys. Condens. Matter 14, L559 (2002)
- [13] A. V. Chubukov, *Phys. Rev. Lett.*, **69**, 832 (1992).
- [14] D. A. Huse and A. Rutenberg, *Phys. Rev. B*, **45**, 7536 (1992).
- [15] E. P. Chan, Ph. D. thesis (Cornell Univ., 1994); C. L. Henley and E. P. Chan, J. Mag. Mag. Mater. 140-144, 1693 (1995).
- [16] I. Ritchey, P. Coleman and P. Chandra, *Phys. Rev. B*, **47**, 15342 (1993).
- [17] G. Chartrand and P. Zhang, *Introduction to Graph Theory* (McGraw-Hill, New York, 2005), chapter 10.
- [18] J. M. Hopkinson and H.-Y. Kee, Phys. Rev. B 74, 224441 (2006).
- [19] U. Hizi and C. L. Henley, Phys. Rev. B 73, 054403 (2006)
- [20] D. L. Bergman, R. Shindou, G. A. Fiete, and L. Balents, Phys. Rev. B 75, 094403 (2007).
- [21] C. L. Henley, unpublished.
- [22] E. F. Shender and P. C. W. Holdsworth, *J. Phys. Cond. Matt.*, **7**, 3295 (1995).
- [23] D. A. Huse, W. Krauth, R. Moessner, and S. L. Sondhi, Phys. Rev. Lett. 91, 167004 (2003).
- [24] C. L. Henley, Phys.Rev. B 71, 014424 (2005).
- [25] S. V. Isakov, K. Gregor, R. Moessner, and S. L. Sondhi, Phys. Rev. Lett. 93, 167204 (2004).
- [26] M. Hermele, M. P. A. Fisher, and L. Balents, Phys. Rev. B 69, 064404 (2002).
- [27] C. L. Henley, Phys. Rev. Lett. 96, 047201 (2006).
- [28] U. Hizi, P. Sharma, and C. L. Henley, Phys. Rev. Lett. 95, 167203 (2005); U. Hizi and C. L. Henley, J. Phys. Condens. Matt. 19, 145268 (2007).